OPTO-ELECTRONICS REVIEW **12**(4), 365–368

Growth and scintillation properties of Ce-doped PrF_3 single crystals

K. KAMADA*, A. YOSHIKAWA[1], T. SATONAGA[2], H. SATO[3], A. BEITLEROVA[4], M. NIKL[4], N. SOLOVIEVA[4], and T. FUKUDA[1,3]

[1]Institute of Multidisciplinary Research for Advanced Materials, Tohoku University, 2-1-1 Katahira, Aoba-ku, Sendai 980-8577, Japan
[2]Stella Chemifa Co. Ltd., 3-6-3 Awaji-cho chuo-ku Osaka, Japan
[3]Fukuda Crystal Laboratory Ltd., 6-6-3 Minami-Yoshinari, Aoba-ku, Sendai 989-3204, Japan
[4]Institute of Physics AS CR, Cukrovarnicka 10, 162 53 Prague, Czech Republic

The scintillation characteristics of the Ce-doped PrF_3 single crystals have been studied to find out their potential as for heavy scintillators. Crystal growth was performed in a vacuum-tight micro-pulling down (μ-PD) system. PrF_3 crystal was prepared with various concentrations (0, 0.1, 0.5, 1, 3, 5, 10, 20, 60, 80, 100%) of Ce^{3+}. The crystals were transparent (CeF_3) or of greenish colour, 3 mm in diameter and 15–50 mm in length. Neither visible inclusions nor cracks were observed. At room temperature, the radio- and photoluminescence spectra and the decay kinetics were measured for the sample set.

Keywords: micro-pulling-down method, fluoride, single crystal, luminescence, scintillator, Ce^{3+}.

1. Introduction

Fluoride crystals are interesting host for rare earth ion doping and can be used to develop the scintillator materials. Ce-doped rare-earth fluoride crystals are one of the promising compositions with some very attractive properties for scintillating applications such as high density and fast luminescence due to the Ce^{3+} 4f-5d transition.

CeF_3 single crystals were intensively studied for scintillator application in High Energy Physics in the first half of nineties [1,2]. Lower light yield of this Ce-concentrated system was explained by essentially nonradiative recombination between Ce^{4+} and an electron, interaction between the closely spaced excited Ce^{3+} ions and a limited concentration quenching effect. Luminescence of the neighbouring Pr^{3+} rare earth ion was studied mainly due to its usage in up-conversion or photon cascade emission systems [3,4], but detailed study of PrF_3 single crystal luminescence has not been published to our knowledge. A question arises, which luminescence and scintillation features can be obtained in the Ce-doped PrF_3 crystals.

In this paper, Ce-doped (0, 0.1, 0.5, 1, 3, 5, 10, 20, 60, 80, and 100% of Ce^{3+}) PrF_3 single crystal rods were prepared and their luminescence and scintillation characteristics were studied. Energy transfer processes between the Pr^{3+} and Ce^{3+} ions were evidenced.

*e-mail: pinna@mail.tagen.tohoku.ac.jp

2. Experimental procedure

2.1. Crystal growth and characterization

Starting materials were prepared from the stoichiometric mixture of 99.99% pure CeF_3 and PrF_3 powders produced by Stella Chemifa Corporation. They were well mixed and put into the crucible.

First, a chamber was evacuated up to 10^{-4} torr, and then the crucible was heated up to 600°C. In order to remove oxygen traces due to moisture of raw materials and contaminated chamber surface, it is kept about 1 hour at this temperature. During this baking procedure, chamber is further evacuated down to 10^{-4} torr. After the baking, vacuum system was stopped and high purity Ar (99.999%) was flushed in the chamber. Then, under ambient pressure, crucible was heated up to the melting temperature (1430°C).

Platinum wire was used instead of the seed for the initial crystal growth. Further crystal growth attempts were carried out using the seed of PrF_3 crystal obtained in the initial experiments. The growth rate was 0.05–0.5 mm/min.

Pieces of grown crystals were crashed and ground into powders in the mortar. Powder X-ray diffraction analysis was carried out in the 2θ range 20–80° using RINT Ultima (RIGAKU) diffractometer. X-ray source was $Cu_{K\alpha}$, the accelerating voltage was 40 kV, and the current was 40 mA.

Quantitative analyses of the crystals for Ce and Pr along the growth direction were performed by electron probe micro-analysis (EPMA; JXA-8621MX, JEOL). ZAF correction

is used, where Z is the atomic number, A is the absorption correction factor, and F is the fluorescence correction factor.

2.2. Optical measurements

Luminescence spectra and decay kinetics at room temperature (RT) were measured at Spectrofluorometer 199S (Edinburgh Instrument) using X-ray tube (operated at 35 kV and 16 mA, Mo cathode) and pulsed nanosecond hydrogen-filled flashlamp for the excitation. Single grating excitation and emission monochromators and photon counting detection were employed, for the details see Ref. 5. Absorption spectra were measured at Shimadzu UV 3101 PC absorption spectrometer. Measurements were performed using the polished 0.8-mm thick sample plates obtained from the pulled rods.

3. Result and discussion

3.1. Crystal growth

$(Pr_{1-x}Ce_x)F_3$ (x = 0.0, 0.001, 0.005, 0.01, 0.03, 0.05, 0.10, 0.20, 0.6, 0.8, 1.0) single crystals were grown by the μ-PD method (examples are shown in Fig. 1). Grown crystals were transparent, greenish colour (except colourless CeF_3), 3 mm in diameter and 15–50 mm in length. Neither visible inclusions nor cracks were observed.

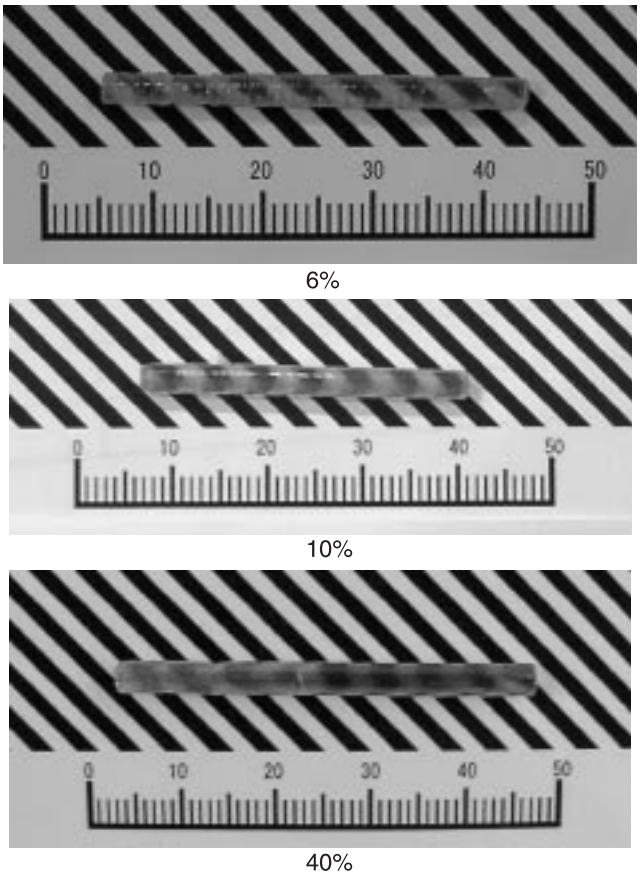

Fig. 1. Photograph of the grown Ce:PrF_3 crystals.

Evolution of powder X-ray diffraction as a function of the Ce^{3+} concentration is shown in Fig. 2(a). No impurity phase was detected and we concluded that PrF_3 and CeF_3 formed a continuous solid solution. As Ce^{3+} concentration increase, the peaks were shifted towards the left. Figure 2(b) shows the lattice constant evolution. It increases linearly as Ce^{3+} concentration increases. Since the ionic radius of Ce^{3+} is larger than that of Pr^{3+}, this tendency is reasonable and it is in good agreement with Vegard's low.

The composition distribution in the grown crystal was observed by EPMA and found to be highly uniform (effective distribution coefficients k_{eff} close to 1). Distribution of Ce^{3+} in $(Ce_{0.2}Pr_{0.8})F_3$ is shown in Fig. 3, as an example. The deviation from the average (calculated) Ce^{3+} concentration within the same crystal did not exceed 2%, which corresponds to the experimental error of the EPMA measurements.

3.2. Luminescent characteristics

Radioluminescence spectra of selected samples are given in Fig. 4. In 0.1% Ce-doped PrF_3 crystal the dominant band at 395 nm and weaker bands at 335 nm and 270 nm are observed and ascribed to the radiative transitions at Pr^{3+} cat-

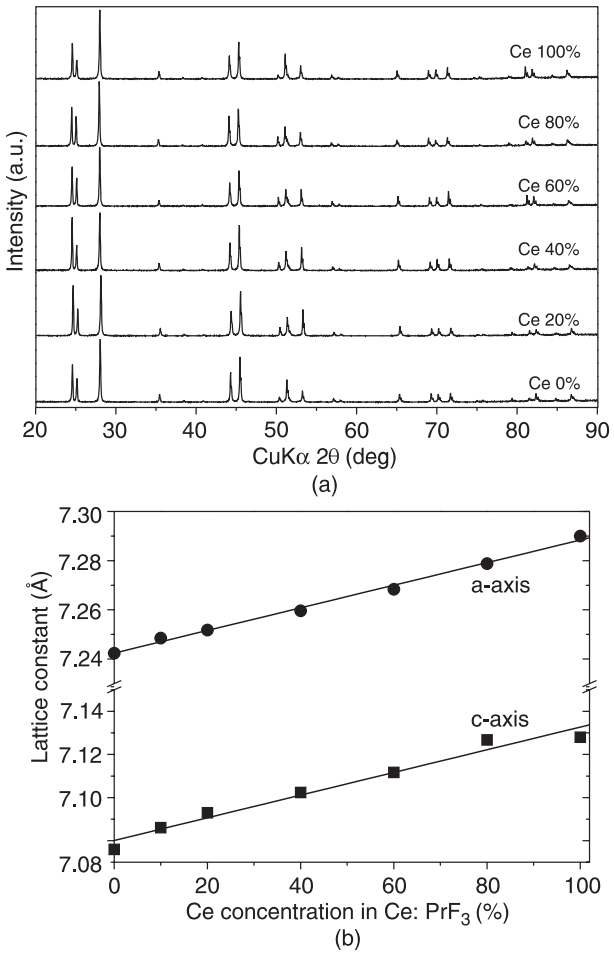

Fig. 2. (a) Evolution of powder X-ray diffraction as a function of Ce^{3+} concentration. (b) Evolution of lattice constant as a function of Ce^{3+} concentration.

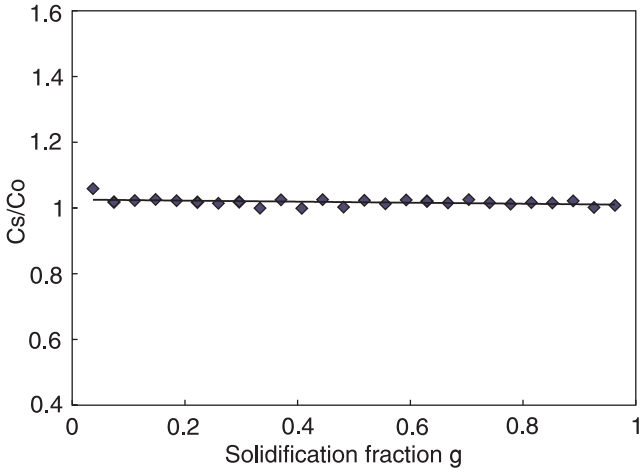

Fig. 3. Distribution of Ce^{3+} in $(Ce_{0.2}Pr_{0.8})F_3$ along the grown crystal.

ion from $^1S_0$ level down to the $^3P_1(^1I_6)$, $^1D_2$ and $^1G_4$ ones, respectively, in agreement with recent published results [6]. With increasing Ce^{3+} concentration intensity of all these emission bands decreases at the expenses of increasing 290-nm band ascribed to the Ce^{3+} centre. Position of the emission spectrum and the value of the decay time (see below) related to the Ce^{3+} emission centre is closely similar to that found in LaF_3:Ce or CeF_3 itself [1,2,7]. Decreasing intensity of the 290 nm band for Ce:PrF_3 (20%) probably indicates an onset of concentration quenching. Concentration dependence of the luminescence spectra points to the competition in energy capture between the Ce^{3+} or Pr^{3+} ions. For completeness, the absorption spectrum of 0.5% Ce-doped PrF_3 is given in Fig. 4 and observed absorption peaks ascribed to transitions at Pr^{3+} and Ce^{3+} ions. Apparently, the Ce^{3+} emission cannot be re-absorbed by any absorption transition of Pr^{3+} ions. Photoluminescence decay kinetics was measured in the 395-nm band under the 215-nm excitation (expected transition $^3H_4$–$^1S_0$). Photoluminescence decay curves normalized to the unity are given in Fig. 5 for the undoped, 1% and 3% Ce-doped samples. Pronounced shortening of the decay together with the concentration dependence of emission spectra in Fig. 4 points to the nonradiative energy transfer from Pr^{3+} to Ce^{3+} ions, most probably from $^1S_0$ state of Pr^{3+} to the higher 5d states of Ce^{3+}. For Ce-concentrations round 3%, the 395 nm emission decay becomes comparable with that of the Ce^{3+} 290 nm band (18 ns decay time, also in Fig. 5). The spectrally unresolved scintillation decay curve at room temperature of Ce1 and 3% doped PrF_3 are given in Fig. 6. The 3% Ce-doped PrF_3 sample shows nearly single exponential decay of 20.5 ns decay time, which is coherent with the photoluminescence decay kinetics in Fig. 5. Such similarity point to negligible occurrence of shallow traps and retrapping processes, which are usually responsible for slower decay components. For 1% Ce sample the dominant decay time is of 32.2 ns, which is due to still slower decay of Pr^{3+} emission in the 395-nm band (Fig. 5). In the 20%

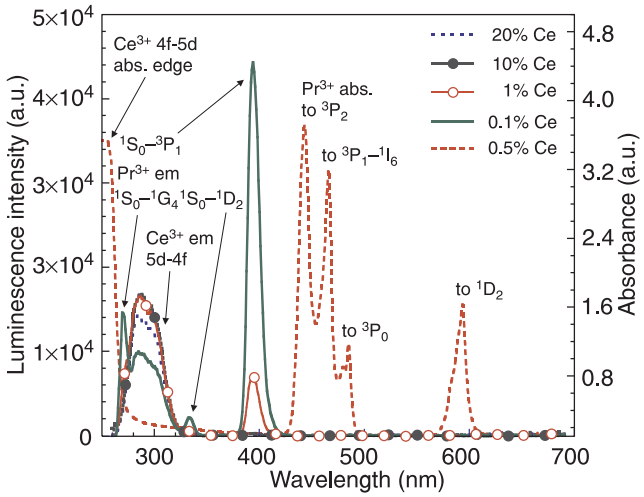

Fig. 4. Radioluminescence spectra of Ce: PrF_3 (0.1, 1, 10, and 20% of Ce^{3+}) at room temperature. Absorption spectrum of Ce:PrF_3(0.5%) is also given in the figure.

Ce-doped PrF_3 (not shown) scintillation decay is further shortened (about 10 ns) with respect to Ce^{3+} intrinsic lifetime (about 18–19 ns) most probably due to the onset of the concentration quenching. From preliminary comparison of radioluminescence intensity it seems that the integral scintillation efficiency of CeF_3 and PrF_3:Ce (1–10%) is comparable.

4. Conclusions

Ce doped PrF_3 single crystal rods with no visible defects could be grown by the μ-PD method. The compositional homogeneity of the Ce-doped PrF_3 single crystals was evidenced. Radioluminescence spectra feature the emission bands of Pr^{3+} at the 395, 335, and 270 nm for undoped or weakly Ce-doped samples, which arise due to $^1S_0 \rightarrow {}^3P_1, {}^1D_2$ and $^1G_4$ transitions at Pr^{3+} ions, respectively.

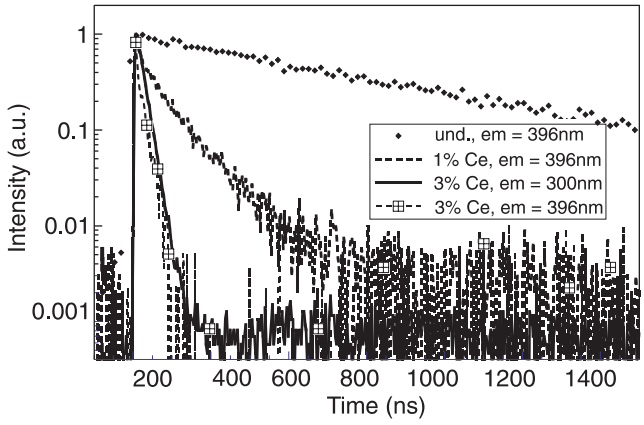

Fig. 5. Normalized decay curves of the 396-nm emission (exc = 215 nm) of Pr^{3+} in the undoped, 1% and 3% Ce-doped PrF_3 is shown. For Ce:PrF_3 (3%), emission decay of Ce^{3+} luminescence at 300 nm is also given under the 250 nm excitation.

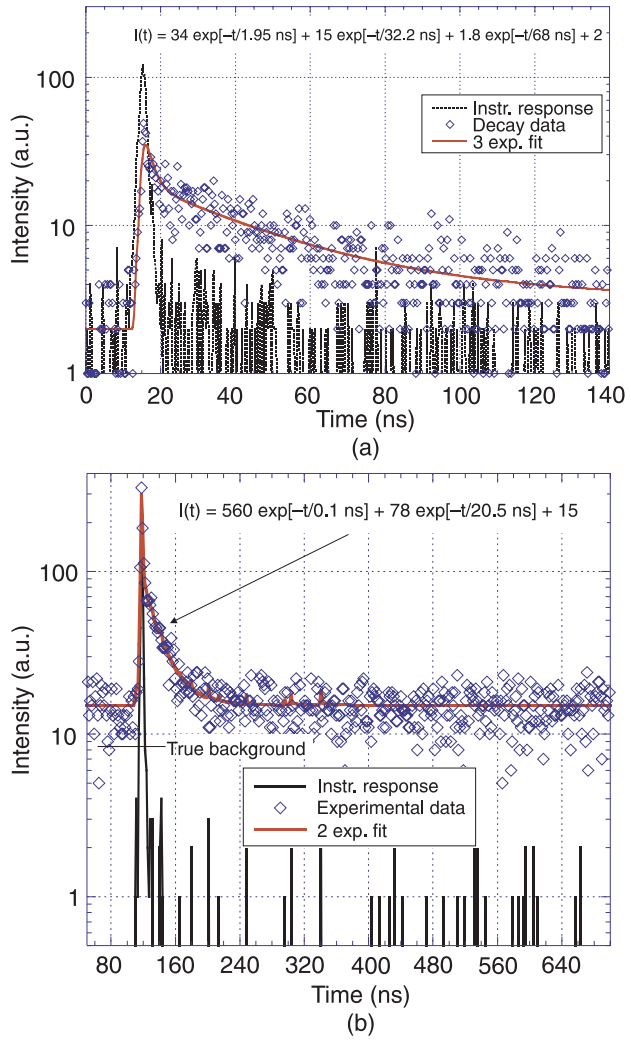

Fig. 6. Spectrally unresolved scintillation decay of 1% (a) and 3% (b) Ce-doped PrF_3 crystal at 295 K under excitation by 22Na radioisotope (511 keV photons). Instrumental response to a Δ-excitation (direct hit of 511 keV photons to photocathode) is also provided by a dashed line. Scintillation decay is approximated by a convolution between the instrumental response and a (2–3)-exponential function. The shortest component (decay time below 2 ns) is due to the direct hit of 511 keV photons onto the detection photomultiplier and does not have any physical significance.

In heavily doped samples only the Ce^{3+} emission at 290 nm is observed with about 18-ns intrinsic lifetime. Energy transfer from Pr^{3+} to Ce^{3+} ions results in shortening decay time of Pr^{3+} luminescence mentioned (about 580 ns in the undoped PrF_3) down to 20.2 ns for concentration of Ce^{3+} of about 3%. For this Ce concentration the scintillation decay is closely similar to the photoluminescence one and reflects mainly the decay times of the Pr^{3+} and Ce^{3+} emission centres with negligible amount of any other slower components.

Acknowledgements

Authors would like to thank to Mr. Murakami, of the Laboratory for Developmental Research of Advanced Materials in IMR, for his assistance with the EPMA analysis. Authors also would like to thank to technical services section in IMRAM with designing and making carbon crucibles for crystal growth.

This work was partially supported by the Industrial Technology Research Grant Program in 03A26014a from New Energy and Industrial Technology Development Organization (NEDO) of Japan. Partial support of the Czech MSMT, KONTAKT grant 1P2004ME716 is also gratefully acknowledged.

References

1. E. Auffray, *Nucl. Instr. Meth. Phys. Research* **A383**, 367–390 (1996).
2. M. Nikl, *Phys. Stat. Sol. (a)* **178**, 595–620 (2000).
3. A.A. Kaminskii and H.J. Eichler, *Phys. Stat. Sol. (b)* **K85**, (1994).
4. A.P. Vink, P. Dorenbos, J.T.M. de Haas, H. Donker, P.A. Rodnyi, A.G. Avanesov, and C.W.E. van Eijk, *J. Phys. Cond. Matter.* **14**, 8889 (2002).
5. M. Nikl, E. Mihokova, Z. Malkova, A. Vedda, M. Martini, K. Shimamura, and T. Fukuda, *Phys. Rev.* **B66**, 184101 (2002).
6. K. Shimamura, E.G. Villora, S. Nakakita, M. Nikl, and N. Ichinose, *J. Cryst. Growth* **264**, 208 (2004).
7. C. Pedrini, B. Moine, J.C. Gacon, and B. Jacquier, *J. Phys. Cond. Mat.* **4**, 5461 (1992).

